www.lajss.org
Latin American Journal of Solids and Structures 6 (2009) 169–183

2D moving element method for random vibration analysis of vehicles on Kirchhoff plate with Kelvin foundation

W.T. Xu[1], J.H. Lin[1,*], Y.H. Zhang[1], D. Kennedy[2] and F.W. Williams[2]

[1]State Key Laboratory of Structural Analysis for Industrial Equipment Faculty of Vehicle Engineering and Mechanics, Dalian University of Technology, Dalian 116023 – People's Republic of China
[2]Cardiff School of Engineering, Cardiff University, Cardiff CF24 3AA, Wales – U.K.

Abstract

Vehicle-pavement coupling systems may produce random vibration due to the road surface unevenness. In this paper, a Kirchhoff plate with Kelvin foundation is employed to model the pavement system and the one-dimensional moving element method proposed by Koh et al. is extended to deal with the random vibration of two-dimensional vehicle-pavement coupling systems. The plate element stiffness matrix is formulated in a coordinate system which moves with the load and the equation of motion of the coupled system is established. The pseudo excitation method is used to analyze random vibration of the coupled system and the influences on the responses both of the vehicle velocity and of the pavement damping are investigated by using numerical examples. Hence useful conclusions are drawn.

Keywords: vehicle-pavement coupled systems, random vibration, moving element method, pseudo excitation method.

1 Introduction

Coupled dynamic analysis of freeway pavement and moving vehicles is a very important topic for both vehicle manufacture and road construction and so is dealt with in many papers, including the following. The displacement, stress and strain of pavement systems have often been analyzed for static loads [5,15]. However, pavement critical responses can be induced by moving dynamic loads and therefore many studies have sought the dynamic response of pavements subjected to moving loads, either with the moving loads assumed to be constant [7, 16] or taking into account the variations of the load amplitude with time due to pavement surface roughness and the mechanical systems of the vehicles [13, 14]. This paper examines and discusses such dynamic response of vehicle-pavement systems, building on the sound foundations of the papers cited in the next paragraph. Kim and Roesset [9] investigated the steady state response of an infinite plate on an elastic foundation to a harmonic moving rectangular uniform load. Fryba [2] studied dynamical characteristics of an infinite or finite plate for various boundary conditions.

*Corresp. author email: jhlin@dlut.edu.cn Received 20 Oct 2008; In revised form 26 Mar 2009

Kim [8] used a double Fourier transform to investigate the stability and dynamic displacement response of an infinite thin plate resting on either Winkler or two-parameter elastic foundations and subjected to in-plane static compressive forces and a distributed load which moves with a constant velocity. Huang and Thambiratnam [3] developed a procedure which uses the finite strip method to treat the response of rectangular plate structures resting on elastic foundations. Koh et al. [10] proposed a one-dimensional moving element method (MEM) for a train-track system, which is both relatively flexible and quite accurate. Lin et al. [11] used the pseudo excitation method (PEM) to investigate the seismic response of long-span structures subjected to multipoint random ground excitation. Clearly, the random excitation of vehicle-pavement systems is too complicated a problem for an analytical solution to be obtained and conventional finite element methods (FEM) are also not practical because they involve unacceptably large computational effort. Therefore this problem has received much attention. In this paper, the one-dimensional MEM proposed by Koh et al. is extended to two dimensional problems for which the vehicle moves on an infinite Kirchhoff plate supported by a Kelvin foundation. The equation of motion of the vehicle is first derived using a coordinate system which moves with the vehicle, so that the corresponding dynamic problem can be solved as a quasi-static one. It is shown that this gives the element stiffness matrices easily and they are simply the corresponding static element stiffness matrix modified by superposition of terms which account for the velocity effects. Due to the surface unevenness, the responses of the vehicle-pavement coupled systems are evidently random. The pseudo excitation method (PEM) [11,12] is herein used to analyze these random vibration characteristics, and satisfactory results are obtained. Numerical examples are used to investigate phenomena such as the influences of vehicle velocity and pavement damping on responses and some conclusions are drawn which are useful for both vehicle manufacture and road construction.

2 The pavement model and the moving co-ordinate system

A Kirchhoff plate with Kelvin foundation is used as the pavement model (Fig. 1). Its equation of motion can be written as [6]

$$D\nabla^2\nabla^2 u + \mu u + \eta\frac{\partial u}{\partial t} + m\frac{\partial^2 u}{\partial t^2} = p(t)\delta\left(x - Vt\right) \tag{1}$$

where ∇ denotes the Laplacian; $u = u(x, y, t)$ represents the deflection of the plate; $D = Eh^3/12(1-\upsilon^2)$ is the plate flexural rigidity; h, E, υ are the thickness, elastic modulus and Poisson's ratio of the plate; m and $P(t)$ represent its mass per unit area and external load; μ and η denote the rigidity and damping of the foundation and; V is the velocity of the load along the x axis.

For the one-dimensional moving element method (MEM) [10], the elements are formulated in a co-ordinate system attached to the moving vehicle and so are not physical elements attached

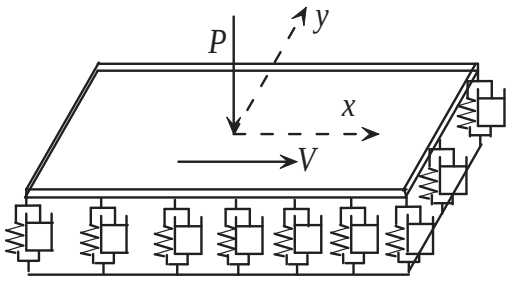

Figure 1: Kirchhoff plate with Kelvin foundation and moving load P.

to the material, but instead are conceptual elements that 'flow' with the moving vehicle along the pavement. The main advantage is that the moving vehicle is static in this coordinate system, which avoids the updating of force or displacement vectors due to change of the contact point with the elements, e.g. it is never necessary to cross from one element into another. In this paper, MEM is extended to investigate 2D problems by using the Kirchhoff plate of Eq.(1) and Fig. 1. A segment of the plate is discretized into a finite number of moving elements (Fig. 2), such that both upstream and downstream ends of the plate segment are sufficiently far from the contact point of the force for the forces and moments there to be negligible.

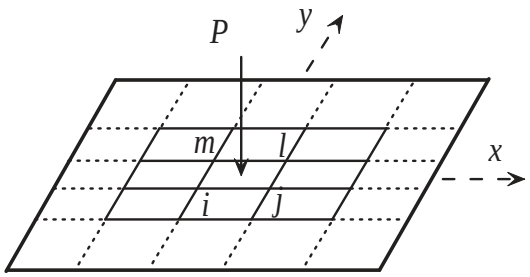

Figure 2: Discretization of plate into moving elements

Now consider a typical moving square element with nodes i,j,m,l and with its moving coordinates (X, Y) defined as

$$X = x - Vt, Y = y \tag{2}$$

The equation of motion of this moving element can be expressed as:

$$\begin{array}{l} D\nabla^2\nabla^2 u + \mu u + \eta\left(\frac{\partial u}{\partial t} - V\frac{\partial u}{\partial X}\right) \\ +m\left(\frac{\partial^2 u}{\partial t^2} - 2V\frac{\partial^2 u}{\partial t \partial X} + V^2\frac{\partial^2 u}{\partial X^2}\right) = p\delta\left(X\right) \end{array} \tag{3}$$

By means of FEM, the deflection u can be expressed in terms of the nodal displacement vector u^e as

$$u = Nu^e \tag{4}$$

where N is the shape function vector. For a Kirchhoff plate element with a Kelvin foundation, the shape function can be written as [1]

$$\mathbf{N} = \left\{ \begin{array}{cccccc} N_i & N_{x_i} & N_{y_i} & N_j & N_{x_j} & N_{y_j} \\ N_m & N_{x_m} & N_{y_m} & N_l & N_{x_l} & N_{y_l} \end{array} \right\}$$

$$N_k = (1+\xi_0)(1+\psi_0)(2+\xi_0+\psi_0-\xi^2-\psi^2)/8$$

$$N_{x_k} = -b\psi_k(1+\xi_0)(1+\psi_0)(1-\psi^2)/8$$

$$N_{y_k} = -a\xi_k(1+\xi_0)(1+\psi_0)(1-\xi^2)/8 \tag{5}$$

$$k = i, j, m, l$$

in which

$$\xi = (x - x_c)/a; \psi = (y - y_c)/b;$$

$$\xi_0 = \xi\xi_k; \psi_0 = \psi\psi_k;$$

where x_c,y_c are the central coordinates of the element, which has length a and width b. Note that most of the elements are not in contact with any loads, so that the force term on the right-hand side of equation (3) vanishes. By using Galerkin's approach, i.e. equation (3) is multiplied by a weighting function (variation) N and integrated over the plate element, the weak Galerkin form can be obtained as

$$\begin{array}{l} \iint_{\mathrm{s}} N[D\nabla^2\nabla^2 u + \mu u + \eta\left(\frac{\partial u}{\partial t} - V\frac{\partial u}{\partial X}\right)] + \\ \iint_{\mathrm{s}} N[m\left(\frac{\partial^2 u}{\partial t^2} - 2V\frac{\partial^2 u}{\partial t \partial X} + V^2\frac{\partial^2 u}{\partial X^2}\right) - p\delta(X)] = 0 \end{array} \tag{6}$$

Substituting Eqs. (4) and (5) into Eq. (6) gives

$$\begin{array}{l} \iint_{\mathrm{s}} \left(B^{\mathrm{T}} D B\right) u^e ds \\ + \iint_{\mathrm{s}} \mu N^{\mathrm{T}} N u^e ds + \iint_{\mathrm{s}} \eta\left(\frac{\partial u^e}{\partial t} N^{\mathrm{T}} N - V\frac{\partial N^{\mathrm{T}}}{\partial X} N u^e\right) ds \\ + \iint_{\mathrm{s}} m\left(\frac{\partial^2 u^e}{\partial t^2} N^{\mathrm{T}} N - 2V\frac{\partial u^e}{\partial t}\frac{\partial N^{\mathrm{T}}}{\partial X} N + V^2\frac{\partial^2 N^{\mathrm{T}}}{\partial X^2} N u^e\right) ds \\ - \iint_{\mathrm{s}} N p\delta(X)\, ds = 0 \end{array} \tag{7}$$

in which the element mass, damping and stiffness matrices in the moving coordinate system are, respectively,

$$\begin{array}{l} K_e = \iint_{\mathrm{s}} B^{\mathrm{T}} D B ds + \mu \iint_{\mathrm{s}} N^T N ds \\ -V\eta \iint_{\mathrm{s}} \frac{\partial N^{\mathrm{T}}}{\partial x} N ds + mV^2 \iint_{\mathrm{s}} \frac{\partial^2 N^{\mathrm{T}}}{\partial x^2} N ds \end{array} \tag{8}$$

$$C_e = \eta \iint_{\mathrm{s}} N^{\mathrm{T}} N ds - 2Vm \iint_{\mathrm{s}} \frac{\partial N^{\mathrm{T}}}{\partial X} N ds \tag{9}$$

$$M_e = m \iint_{\mathrm{s}} N^{\mathrm{T}} N ds \tag{10}$$

in which B is the 3×12 matrix:

$$B = -\begin{bmatrix} \frac{\partial^2 N_i}{\partial x^2} & \frac{\partial^2 N_{x_i}}{\partial x^2} & \frac{\partial^2 N_{y_i}}{\partial x^2} & \cdots & \frac{\partial^2 N_{y_l}}{\partial x^2} \\ \frac{\partial^2 N_i}{\partial y^2} & \frac{\partial^2 N_{x_i}}{\partial y^2} & \frac{\partial^2 N_{y_i}}{\partial y^2} & \cdots & \frac{\partial^2 N_{y_l}}{\partial y^2} \\ 2\frac{\partial^2 N_i}{\partial x \partial y} & 2\frac{\partial^2 N_{x_i}}{\partial x \partial y} & 2\frac{\partial^2 N_{y_i}}{\partial x \partial y} & \cdots & 2\frac{\partial^2 N_{y_l}}{\partial x \partial y} \end{bmatrix}$$

$$D = \frac{Eh^3}{12(1-\upsilon)} \begin{bmatrix} 1 & \upsilon & 0 \\ \upsilon & 1 & 0 \\ 0 & 0 & (1-\upsilon^2)/2 \end{bmatrix}$$

Assembling all element matrices gives the equation of motion of the pavement as

$$M_1 \ddot{u} + C_1 \dot{u} + K_1 u = F_1 \tag{11}$$

where $u = \{ u_1 \quad u_2 \quad ... \quad u_n \}$ is the nodal displacement vector. By using MEM the load velocity, foundation damping and rigidity are all coupled in the element matrices and it is shown that Eq.(11) below can easily be computed because it is linear and time-independent.

3 Random vibration analysis of vehicle-pavement coupling system

Fig. 3 shows a model of the vehicle-pavement coupling system in which the vehicle model has 4 degrees of freedom (DOF), namely: the vehicle body vertical displacement z_c; its rotation in the $x-z$ plane θ; the front wheel vertical displacement w_f and; the rear wheel vertical displacement w_r. The equation of motion of the coupled system in the coordinate system which moves with the vehicle can be written as

$$M^{'} \ddot{d} + C^{'} \dot{d} + K^{'} d = F = F_1 + F_2 \tag{12}$$

which incorporates Eq.(11). Here, d is the displacement vector of the coupled system; F is the excitation vector, which includes two parts: F_1 caused by gravity acting on the vehicle and F_2 caused by the random road surface unevenness. The response induced by F_1 is deterministic and can be computed easily by the two-dimensional moving element method proposed in this paper. Therefore we focus now on the random vibration analysis of the coupled system caused by F_2. It

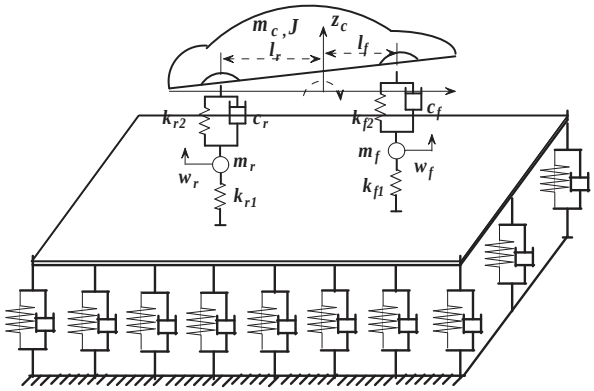

Figure 3: Discretization of plate into moving elements

can be reasonably assumed that F_2 is a stationary Gaussian process with power spectral density (PSD) matrix $S_x^s(\Omega)$ in the spatial domain. According to random vibration theory, the PSD matrix $S_x^t(\omega)$ in the time domain is

$$S_x^t(\omega) = \frac{1}{V} S_x^s(\Omega) \tag{13}$$

and the response power spectrum density (PSD) matrix, $S_{out}(\omega)$, can be computed from

$$S_{out}(\omega) = H^{\mathrm{T}}(\omega) S_x^t(\omega) H(\omega) \tag{14}$$

where $H(\omega)$ is the frequency response matrix. When the system is complicated, using Eq. (14) to obtain $S_{out}(\omega)$ is very time consuming because it involves many matrix inversion and multiplication computations. Therefore it is shown at the end of this section that PEM [12] provides a more efficient way to obtain these response PSDs.

In the vehicle-pavement model the random excitations vectors F_2 can be expressed as

$$F_2(t) = \Gamma R(t) \tag{15}$$

in which: Γ is a matrix which transforms the wheel forces into the element node force vector F_2, which is related to the position of the vehicle and; $R(t)$ is a vector reflecting the road surface unevenness such that

$$R(t) = \{r(t), r(t - \Delta t)\} \tag{16}$$

$$\Delta t = (X_r - X_f)/V$$

Here: $r(t)$ denotes the vertical coordinate of the uneven road surface at the contact point of the front wheel and the plate; X_f and X_r are the contact locations of the front and rear wheels

in the moving coordinate system and; Δt is the time lag between the front and rear wheels. This can be regarded as a fully coherent multi-excitation problem, and PEM can handle it very easily, as follows.

1. Constitute a pseudo harmonic excitation

$$\widetilde{F}_2(t) = \Gamma \left[1, e^{-i\omega\Delta t}\right]^{\mathrm{T}} \sqrt{S_r(\omega)} e^{i\omega t} \tag{17}$$

where $S_r(\omega)$ is the PSD function of $r(t)$.

2. Compute the corresponding harmonic responses

$$\widetilde{d} = H(\omega)\, \widetilde{F}_2(t) \tag{18}$$

where $H(\omega)$ is the frequency response matrix. There is no need to compute $H(\omega)$ because Eq.(18) can be replaced by any process for computing the harmonic responses $\widetilde{d}$.

3. Compute the corresponding PSD

$$S_{\widetilde{d}\,\widetilde{d}}(\omega) = \widetilde{d}^{*} \cdot \widetilde{d}^{\mathrm{T}} \tag{19}$$

in which the time terms $e^{i\omega t}$ and $e^{-i\omega t}$ in $\widetilde{d}^{*}$ and $\widetilde{d}^{\mathrm{T}}$ cancel each other out due to the multiplication, so that $S_{\widetilde{d}\,\widetilde{d}}(\omega)$ is time-independent. It has been proved [11, 12] that Eqs (19) and (14) lead to the same exact solution, but with PEM being much more efficient. After the PSD $S_{\widetilde{d}\,\widetilde{d}}$ has been obtained its standard deviation σ_{d_i} is obtained from

$$\sigma_{d_i}^2 = \int_{-\infty}^{+\infty} S_{d_i d_i} d\omega \tag{20}$$

where $S_{d_i d_i}$ is the PSD of d_i. The above derivation is in the moving coordinate system, so all responses are stationary. Then Eq.(2) is used to obtain the non-stationary standard deviation for a point fixed in the plate.

4 Numerical examples

4.1 Dynamic analysis of a Kirchhoff plate with Kelvin foundation

Consider a constant force moving with steady velocity V along the x axis ($y = 0$) of a smooth plate. The computational parameters are: $E = 1.516\times10^{10}Pa$,$\upsilon = 0.35$,$m = 3.66\times10^{2}\mathrm{kg}/m^2$,$h = 0.15m$, $\mu = 9.5 \times 10^{7}N/m^3$,$P = 2.0 \times 10^{3}N$,$a = 60m$,$b = 20m$.

The segment of the plate is divided into 60×20 moving elements of size $1m \times 1m$. As the excitation is a constant force, the response is time invariant in the coordinate system which moves with the load. As all time derivative terms in equation (11) vanish, no time integration is necessary even though the response is still dynamic at any point of the plate which is located

with respect to the fixed coordinates. Fig. 4 shows how the deflections of the plate vary along the x axis when there is no damping, $V = 27.78$m/s and the vehicle is at $x = 0$. The solid line represents the results obtained using the present method (MEM) and the discrete points represent the results computed by applying the Newmark method in the fixed coordinate system. The agreement is excellent and so verifies the present method.

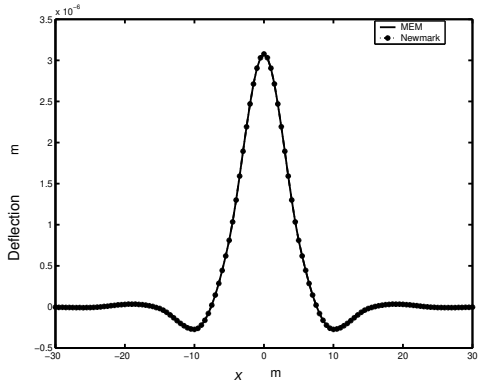

Figure 4: Plate displacement profile for Example 1

Fig. 5 shows the three-dimensional deflected shape of the plate when $t = 0$, i.e. when the force is located at the origin of coordinates. Figs. 5(a) and (b) show the deflected shapes when $V = 27.78m/s$ and $55.56m/s$, respectively, without foundation damping. Clearly, their deflected shapes are symmetrical about both the x and y axes, with the peak value being $3.085 \times 10^{-6}m$ for (a) and $3.572 \times 10^{-6}m$ for (b), so that doubling the velocity caused it to increase by 15.8%. The velocity for Fig. 5(c) is the same as that for Fig. 5(b), but now there is foundation damping with $\eta = 1400kN.s/m^3$. The peak value of (c) is only $1.043 \times 10^{-6}m$. The steady state responses of the plate in the moving co-ordinate system are identical, except for a factor V, to the time-history curves of a fixed point on the plate. So although this paper only gives the deformation curves, the time-history curves can readily be derived from them. Fig. 6 shows the responses of the plate for different damping coefficients and clearly the maximum deflection does not appear where the force is (i.e. $x = 0$), but instead is slightly behind it, as is most evident for heavier damping. For constant load velocity, foundation damping will be the dominant factor influencing the peak value location, as previously observed [6].

Fig. 7 shows the responses for different velocities and damping coefficient $\eta = 1400$ kN.s/m^3. It shows that again these curves are asymmetric, with the peak value occurring slightly behind the force to an extent which increases as the velocity increases.

To investigate the effect of load velocity and foundation damping more extensively, Ref. [3] defines the critical plate velocity $V_{cr} = \left(\frac{4\mu D}{m^2}\right)^{\frac{1}{4}}$, the critical foundation damping $\eta_{cr} = 2\sqrt{\mu m}$, and the dimensionless parameters $\theta = \frac{V}{V_{cr}}$ and $\zeta = \frac{\eta}{\eta_{cr}}$. Fig. 8 uses these parameters to illustrate the influence of load velocity for five alternative foundation damping coefficients. When the

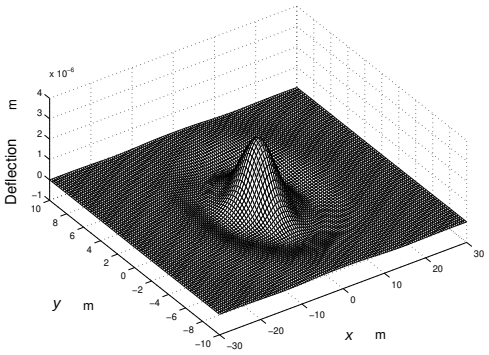

(a) $V = 27.78m/s, \eta = 0$

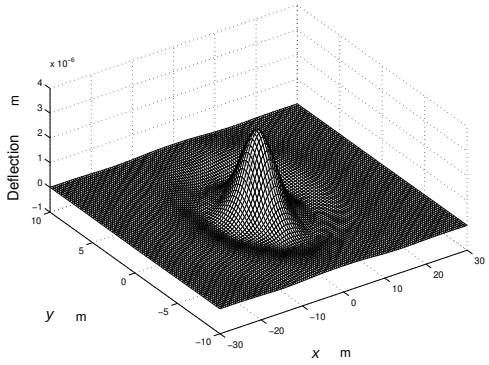

(b) $V = 55.56m/s, \eta = 0$

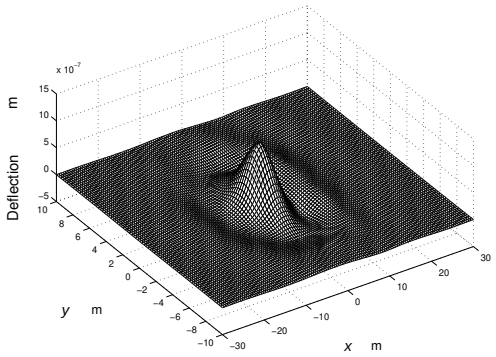

(c) $V = 55.56m/s, \eta = 1400kN.s/m^3$

Figure 5: Three dimensional deflected shape of the plate

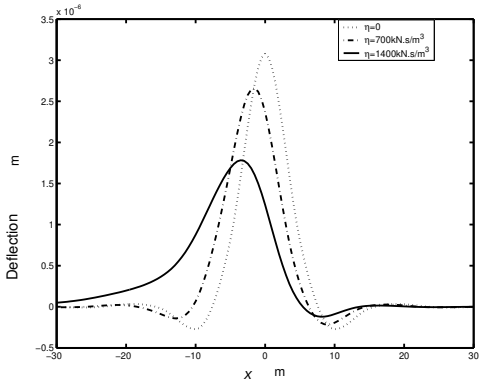

Figure 6: Deflected shapes along x axis for three values of foundation damping

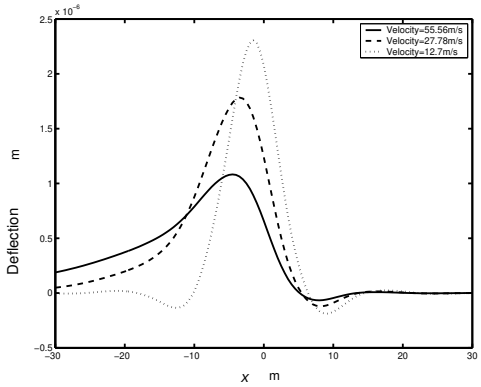

Figure 7: Deflected shapes along x axis for three vehicle velocities

foundation damping is smaller than the critical damping (e.g. $\zeta = 0.5$), the change of the plate response is not pronounced, because it increases slowly with velocity until $\theta \cong 1$ and then decreases. When the foundation damping is bigger than the critical damping, (e.g. $\zeta = 1.5$ or $\zeta = 2.0$), the responses decrease very rapidly with increasing velocity, so that the maximum response occurs for $V = 0$.

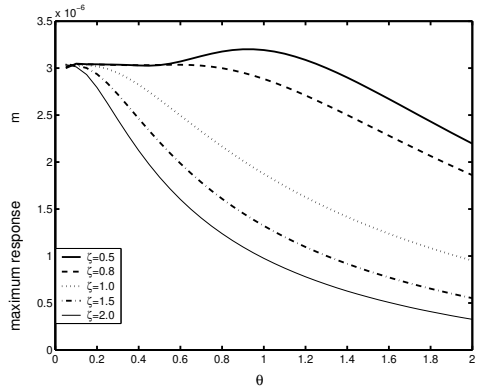

Figure 8: Variation of maximum response with velocity

4.2 Coupled random vibration analysis of a vehicle-pavement system

Using the definitions of Fig. 3 and the pavement parameters of Example 1, let the parameters of a 4-DOF vehicle model [17] be: $m_c = 708\text{kg}$,$m_r = m_f = 80\text{kg}$,$J = 1060\text{kg.m}^2$,$k_{r2} = 19326N/m$, $k_{f2} = 20292N/m$,$c_r = c_f = 1000N.s/m$,$l_r = 1.308m$,$l_f = 1.168m$,$k_{r1} = k_{f1} = 128760N/m$.

The PSD function for the road surface unevenness given by the national standard code (GB7031) [4, 17] is adopted. In the frequency domain this function can be expressed as:

$$S_x^t(\omega) = 2\pi G_q n_0^2 \frac{V}{\omega^2}$$

where n_0 is a reference frequency which is given the usual value $0.1m^{-1}$, while G_q is a coefficient related to the road grade ($16 \times 10^{-6} m^2/m^{-1}$for grade A, $64 \times 10^{-6} m^2/m^{-1}$ for grade B and $256 \times 10^{-6} m^2/m^{-1}$ for grade C).

For road grade C and three different velocities, Fig. 9 gives the PSD functions of the vertical and rotational accelerations of the vehicle body and the vertical accelerations of the front and rear wheels. The peak values of the three response curves shown in Fig. 9(a) always appear at $1.19Hz$, which is the vehicle fundamental frequency, and are higher for higher vehicle velocity. Note that there are also much lower secondary peaks near $6Hz$, the second natural frequency of the vehicle. The vehicle rotational acceleration PSD curves of Fig. 9(b) behave similarly to those of Fig. 9(a) except that now the peaks at the second natural frequency of the vehicle can be higher than those at its fundamental frequency. It would be expected that the peaks for front and rear wheel vertical acceleration PSD should appear at the natural frequencies of the vehicle body and this is indeed true, although the peaks at the first natural frequency are too small to appear to the scale of Figs. 9(c) and (d).

Fig. 10 gives the time-dependent standard deviation curves for vertical displacement of an arbitrary point fixed in the pavement, with the abscissa being the distance from this point to the center of gravity of the vehicle. Clearly, velocity affects the pavement responses only very mildly.

Fig. 11 shows the PSD curves for the same responses as for Fig.9, but now the road grade is varied at constant velocity $55.56m/s$. Clearly, the road condition affects all of these PSD curves very considerably, e.g. for Fig. 11(a) the PSD peak values for road grades C, B and A are in the approximate ratios $16 : 4 : 1$. Fig. 12 corresponds to Fig. 10, except it gives the time-dependent standard deviation curves for the displacement of an arbitrary fixed point on the pavement and clearly shows that the influence of road grade on pavement response is very limited indeed.

5 Conclusions

A computational model has been established for a vehicle-pavement coupled system in a coordinate system which moves with the vehicle. The stiffness matrix has been formulated in this coordinate system, and hence a 2D moving element method has been established to deal with the vehicle-pavement coupled vibration problem. The pseudo excitation method has then been used to analyze the random vibration characteristics, and useful results have been obtained, as follows.

1. The responses of the plate are influenced by the Kelvin foundation damping coefficient, the plate parameters and the load velocity. The influences of the foundation damping coefficient and load velocity on the variation of the deflected shape with x are asymmetric, and are increasingly

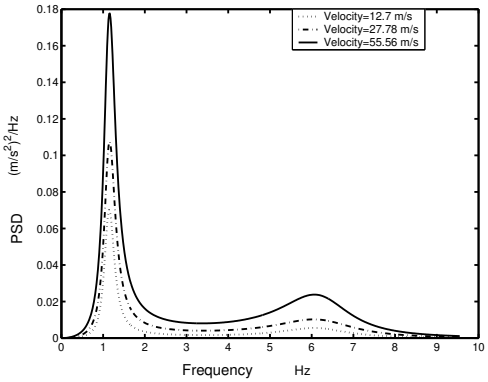

(a) Vehicle body vertical acceleration PSD

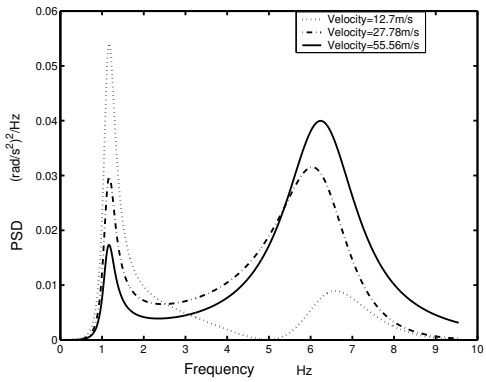

(b) Vehicle body rotational acceleration PSD

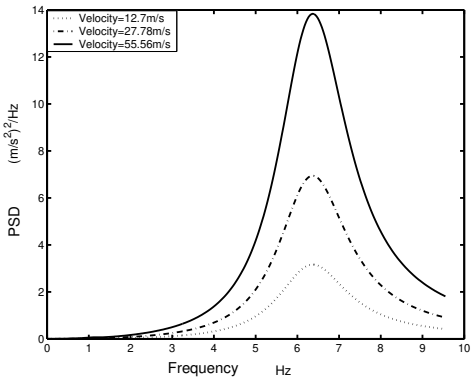

(c) Front wheel vertical acceleration PSD

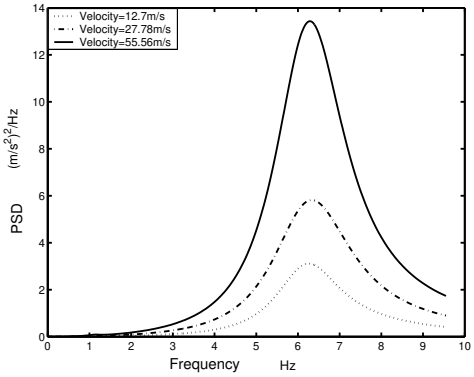

(d) Rear wheel vertical acceleration PSD

Figure 9: PSDs for vehicle component accelerations

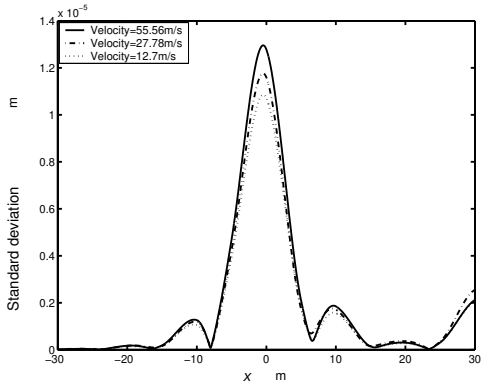

Figure 10: Standard deviation for pavement vertical displacement

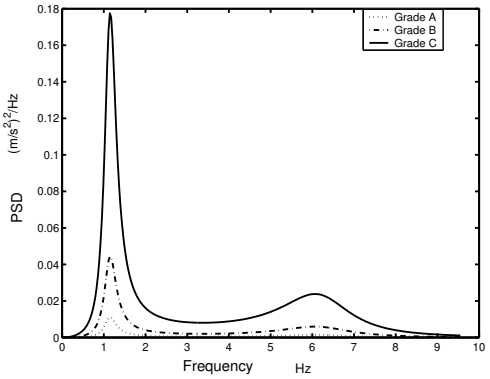

(a) Vehicle body vertical acceleration PSD

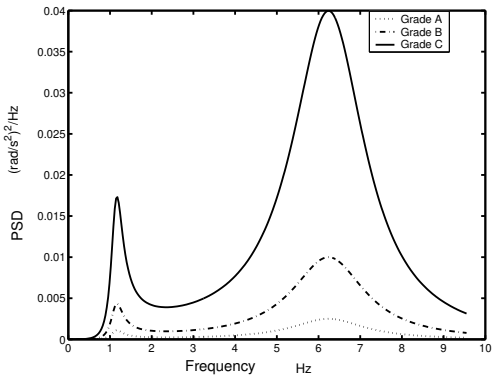

(b) Vehicle body rotational acceleration PSD

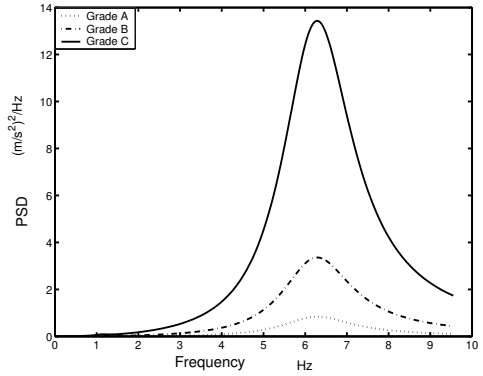

(c) Front wheel vertical acceleration PSD

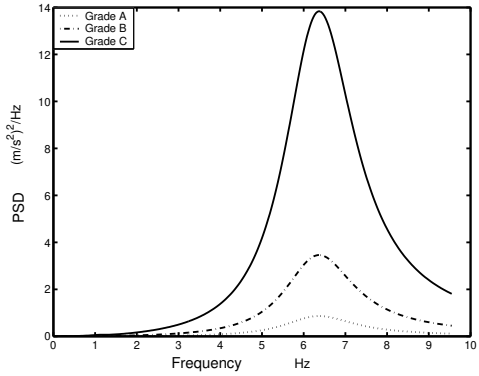

(d) Rear wheel vertical acceleration PSD

Figure 11: PSDs for vehicle component accelerations

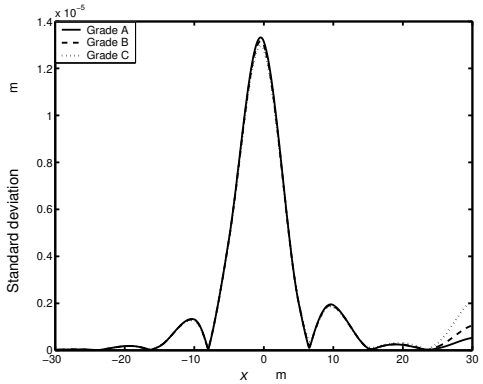

Figure 12: Standard deviation for pavement vertical displacement

so as the load velocity increases.
2. For different foundation damping coefficients, the effects of the load velocity on the midpoint responses of plate differ qualitatively. Thus for smaller damping coefficients, the peak value of a midpoint response appears when the load velocity V is equal to the critical plate velocity, whereas for bigger damping coefficients it appears when $V = 0$.
3. For vehicle-pavement coupled systems, resonance appears when the excitation frequency is close to the vehicle natural frequencies. For a given road grade, the vehicle velocity is the main factor governing the vehicle vibration; whereas at constant velocity the influence of the grade of the road surface unevenness has a major effect on vehicle vibration. However, pavement displacement is almost completely governed by load on the vehicle.

Acknowledgment

The writers are grateful for the financial support from the Natural Science Foundation of China (90815023), from the National High Technology Research and Development Program of China (2007AA11Z101).

References

[1] R.D. Cook, D.S. Malkus, M.E. Plesha, and R.J. Witt. *Concepts and Applications of Finite Element Analysis*. John Wiley & Sons, New York, 4 edition, 2001.

[2] L. Fryba. *Vibration of solid and structures under moving loads*. Thomas Telford, London, 1999.

[3] M.H. Huang and D.P. Thambiratnam. Deflection response of plate on winkler foundation to moving accelerated loads. *Eng. Struct.*, 23(9):1134–1141, 2001.

[4] W. Huang, Y.Q. Zhao, and G.Q. Yang. Pseudo excitation method for vehicle dynamic loads calculation. *Tractor & Farm Transporter*, 33(2):19–23, 2006. (in Chinese).

[5] Y.H. Huang. *Pavement analysis and design*. Prentice Hall, New Jersey, 1993.

[6] J.Q. Jiang and H.F. Zhou. Steady state response of infinite plate on visco-elastic foundation subjected to moving load. *China Journal of Highway and Transport*, 19(1):6–11, 2006. (in Chinese).

[7] E. Kausel and J.M. Roesset. Frequency domain analysis of undamped systems. *J. Eng. Mech.*, 118(4):721–732, 1992.

[8] S.M. Kim. Buckling and vibration of plate on elastic foundation subject to in-plane compression and moving loads. *Int. J. Solids Struct.*, 41(20):5647–5664, 2004.

[9] S.M. Kim and J.M. Roesset. Moving loads on a plate on elastic foundation. *J. Eng. Mech.*, 124(9):1010–1017, 1998.

[10] C.G. Koh, J.S.Y. Ong, D.K.H. Chua, and J. Feng. Moving element method for train-track dynamics. *Int. J. Numer. Meth. Engrg.*, 56(10):1549–1567, 2003.

[11] J.H. Lin, J.J. Li, W.S. Zhang, and F.W. Williams. Structural seismic response to inhomogeneous random field. *Eng. Comput.*, 14(7):718 –734, 1997.

[12] J.H. Lin, Y. Zhao, and Y.H. Zhang. Accurate and highly efficient algorithms for structural stationary/non-stationary random response. *Comput. Methods Appl. Mech. Engrg.*, 191(1-2):103–111, 2001.

[13] M.A. Nasim, S.M. Karamihas, T.D. Gillespie, W. Hansen, and D. Cebon. Behavior of a rigid pavement under moving dynamic loads. *Transportation Research Record*, 1307:129–135, 1991.

[14] R.V. Siddharthan, J. Yao, and P.E. Sebaaly. Pavement strain from moving dynamic 3D load distribution. *J. Transp. Eng.*, 124(6):557–566, 1998.

[15] H.M. Westergaard. *Stresses in concrete pavements computed by theoretical analysis.* Public Roads, 1925.

[16] S.M. Zaghloul and T.D. White. Use of three dimensional dynamic finite element program for analysis of flexible pavement. *Transportation Research Record*, 1388:60–69, 1993.

[17] L.L. Zhang, J.S. Tang, and L.B. Li. Transient dynamic response analysis of a thin-walled conical shell. *Journal of Vibration and Shock*, 25(6):168–187, 2006. in Chinese).